



The CDF Central Electromagnetic Calorimeter*

L. Balka, K. Coover, R. Diebold, W. Evans, N. Hill, L. Nodulman,
J. Proudfoot, R. Rezmer, J. R. Sauer*, P. Schoessow, and D. Underwood
R. G. Wagner, E. Walschon, and A. B. Wicklund
Argonne National Laboratory, Argonne, Illinois 60439 USA†

T. Kamon, Y. Kikuchi, K. Kondo, K. Takikawa, and A. Yamashita
University of Tsukuba, Sakura-mura, Niihari-gun, Ibaraki-ken, 305, Japan

J. E. Elias, H. Jensen, H. Kautzky, R. Krull, and K. Yasuoka
Fermi National Accelerator Laboratory, Batavia, Illinois 60510 USA

T. Devlin and U. Joshi
Rutgers University, New Brunswick, New Jersey 08903 USA

D. Bauer**, D. Connor, J. W. Cooper***, S. R. Hahn, M. Miller,
R. VanBerg, and H. H. Williams‡
University of Pennsylvania, Philadelphia, Pennsylvania 19104 USA

S. Kobayashi and A. Murakami
Saga University, Honjo-cho 1, Saga-shi 840, Japan

S. Mikamo
National Laboratory for High Energy Physics, KEK, Oho-machi, Tsukuba-gun, Ibaraki-ken, 305, Japan

July-August 1987

*Submitted to Nucl. Instrum. Methods A



THE CDF CENTRAL ELECTROMAGNETIC CALORIMETER

L. BALKA, K. COOVER, R. DIEBOLD, W. EVANS, N. HILL, L. NODULMAN,
J. PROUDFOOT, R. REZMER, J.R. SAUER*, P. SCHOESSOW, D. UNDERWOOD,
R.G. WAGNER, E. WALSHON, and A.B. WICKLUND
Argonne National Laboratory, Argonne, Illinois 60439 USA †

T. KAMON, Y. KIKUCHI, K. KONDO, K. TAKIKAWA, and A. YAMASHITA
University of Tsukuba, Sakura-mura, Niihari-gun, Ibaraki-ken 305, Japan

J.E. ELIAS, H. JENSEN, H. KAUTZKY, R. KRULL, and K. YASUOKA
Fermi National Accelerator Laboratory, Batavia, Illinois 60510 USA

T. DEVLIN and U. JOSHI
Rutgers University, New Brunswick, New Jersey 08903 USA

D. BAUER**, D. CONNOR, J.W. COOPER***, S.R. HAHN, M. MILLER,
R. VANBERG, and H.H. WILLIAMS ‡
University of Pennsylvania, Philadelphia, Pennsylvania 19104 USA

S. KOBAYASHI and A. MURAKAMI
Saga University, Honjo-cho 1, Saga-shi 840, Japan

S. MIKAMO
National Laboratory for High Energy Physics, KEK, Oho-machi, Tsukuba-gun, Ibaraki-ken 305, Japan

The central electromagnetic calorimeter for the Collider Detector at Fermilab uses a hybrid design with scintillator and wavelength shifter for energy measurement and an embedded strip chamber for position determination and longitudinal shower development. Complementary calibration systems are incorporated in the design. Calorimeter characteristics and performance are summarized. An average energy resolution, $\sigma(E)/E$, of $13.5\%/\sqrt{E \sin \theta}$ (with E in GeV), and a position resolution of ± 2 mm at 50 GeV are measured.

⁺Work supported in part by the U.S. Department of Energy, Division of High Energy Physics, Contract W-31-109-ENG-38.

[†]Work supported in part by the U.S. Department of Energy, Division of High Energy Physics, Contract DE-AC02-76-ERO-3071.

1. Introduction

The hybrid (scintillator plus strip chamber) design used for the CDF central electromagnetic (E-M) calorimeter was developed in order to combine the good resolution of scintillator with the fine segmentation of one or more gas layers [1,2]. The results of testing a full scale calorimeter prototype as well as subsequent design changes for production are given in Reference [3]. A description of the production modules and their performance in tests follows. Central E-M calorimeter characteristics are summarized in Table 1.

2. Mechanics

The basic layout of each module is shown in Figures 1 and 2. An inner aluminum base plate begins the central E-M calorimeter at a perpendicular radius of 68 in. from the beam line. Its nominal 1 in. thickness is reduced in pockets down to $\frac{3}{8}$ in. The average thickness has only 0.55 in. of aluminum. Thirty-one layers of 5 mm thick SCSN-38 polystyrene scintillator [4] are cut and polished on the interior sides. Individual pieces are wrapped in two layers of 0.0015 in. vellum drawing paper. The pieces are assembled to form ten projective towers, each subtending 0.10 units of pseudorapidity and 15° in ϕ . Interleaved with the scintillator are 30 layers of $\frac{1}{8}$ in. lead, clad on both sides with 0.015 in. aluminum. Wavelength shifters fit into a gap between the machine finished surface of the stack and $\frac{3}{16}$ in. thick steel cover plates, one on each side for two per tower. The gap is 0.25 ± 0.02 in. thick. The skins and gaps represent 4.8% of the azimuth. A proportional strip chamber is inserted inside the stack between the eighth lead layer and the ninth scintillator layer, at the depth corresponding to maximum average

transverse shower development.

In order to maintain a constant radiation length thickness as polar angle varies, both up to the strip chamber and total, acrylic is substituted for lead in certain layers for towers as shown in Figure 1. The sides of scintillator behind acrylic are painted black. A given layer of scintillator is cut contiguously from a parent casting with thickness measurements retained. The parent castings are sorted into layers to give a uniform total thickness and profile to stacks. The total stack thickness, held under 20 PSI for machining, is kept to 12.6 ± 0.1 in. by selective insertion of layers of 0.01 in. Mylar. A typical stack contains about 0.4 in. of Mylar. When mounted into the wedge module the stack is held against the aluminum base plate by a box spring pushing against the innermost iron calorimeter layer at about 3 PSI. The stack begins $\frac{5}{8}$ in. inside the 1 in. iron 90° end plate in order to allow mechanical connection to the lead. At the 45° end there is a 2 in. gap to the 1 in. stainless steel end plate to allow space for light gathering. Table 2 lists central E-M calorimeter tower thicknesses at their midpoints.

One wedge module is notched to allow a "chimney" for access to the CDF superconducting solenoid. The E-M calorimeter of that wedge is 12 in. shorter than usual, with seven normal towers and one combined tower; thus, the total number of phototubes used in the central E-M calorimeters is $48 \text{ modules} \times 10 \text{ towers per module} \times 2 \text{ phototubes per tower} - 2 \text{ "chimney" towers} \times 2 \text{ phototubes per tower} = 956$. The gap from the stack to the 45° end plate in this module is 0.75 in. as no space is required for lightguides.

3. Light Collection

The blue light from the scintillator is collected in 3 mm thick UVA acrylic doped with 30 ppm Y7 from Kyowa Gas Chemical[4]. The waveshifters are laser cut with notches to form 1 in. wide fingers which are bent and gathered to glue to 24 mm by 25.4, 28.6, or 38.1 mm UVA acrylic rod light guides which pass through the hadron calorimeter. The seven towers closest to 90° have their lightguides chamfered $\frac{1}{4}$ in. on the inside smaller angle corner in order to pass between hadron calorimeter scintillators. The light gathering layout is shown in Figure 2, with the light from the scintillator layers being redirected by the two waveshifters on each side up through the lightguides into the two phototubes per tower. The ends of the rods are glued to rectangular-to-round 10 ppm Y7 doped transition pieces. PMTs are aligned to the lightguides by an inner PVC cylinder attached to the magnetic shield. The tower boundary gap between waveshifters is nominally $\frac{1}{4}$ in. total. In mounting, the waveshifters are centered to ± 1 mm. The width of a waveshifter can vary by up to ± 2 mm due to variable shrinkage during annealing. A thirty point waveshifter response map of each assembly was taken for quality control. Response of a given shape of waveshifter is reproducible to $\pm 2\%$ in the transverse first moment (transverse asymmetry corresponding to center to edge difference less than 2%). An online mapping program provided first and second moments of the response in two coordinates and supplied detailed plots when desired. The excitation source for the mapping was light from a piece of actual calorimeter scintillator, excited by a U.V. lamp. The detector at the end of the light pipe was a vacuum photodiode, made from a calorimeter phototube, with electronic amplification for

stability. Absolute light yield varies by 25% rms.

With no corrections, the light output from individual wavelength shifters varies from point to point on its collecting face by as much as 45%. There are two reasons for this: first, the combination of oblique and obtuse angles between edges for a projective geometry shape give differences in collection by total internal reflection. Second, the effective attenuation length of the fingers of about 80 cm causes different transmission through fingers which vary in length from 15 cm to 45 cm. The thickness of the shifter material was controlled to better than 10% in order to have uniform attenuation length, and great effort went into developing the laser cutting technique to give uniform optical surfaces. We used a combination of two techniques to reduce the non-uniformities to no more than $\pm 3\%$. First, the edge of the shifter farthest from the collection fingers was sanded and painted black to eliminate reflection. Second, a backing of controlled reflectivity was used to eliminate the remaining 25% variations. This backing utilized the fact that 25% of the scintillator light passed through the 3 mm shifter material and could be selectively absorbed or reflected back into the shifter to produce more green light. The backings were different for each of the ten tower shapes and consisted of black ink patterns silk screened onto reflective Alzak aluminum. In order to develop the patterns, response maps of each of 20 shifters for 15 wedges were averaged after culling defective assemblies.

4. Photomultiplier Tubes

The green waveshifted light is viewed by 1.5 in. diameter bialkali 10 stage photomultiplier tubes. A set of specifications, summarized in Table 3, was

drawn up based on the UA2 experience as confirmed with small sample tests. A request for proposals resulted in the selection of the Hamamatsu R580. Tubes were burned in and tested against specifications in batches of 20 for about a week before installation as described in Reference [5]. The base circuit, shown in Figure 3, draws about $300 \mu\text{A}$ at approximately 1000 V giving a gain of about 10^5 . The tube mounting has a soft iron outer shield 2.75 in. OD, 2.0 in. ID and 8 in. long. A standard commercial inner shield is attached inside with PVC cylinders. This shielding scheme was tested to make tube gain insensitive to axial magnetic fields of up to 200 Gauss. A mounting spring loads the tube against the lightguide (air junction) and allows for twist-off removal of tube and base, with azimuthal alignment. Photomultiplier high voltages are set and read back by a system of computer controlled DC motor driven potentiometers in series with the bases.

Photomultiplier readout[6] saturates at about 350 GeV and has a high gain ($\times 16$) readout for good pedestal systematics for minimum ionizing particles (about 300 MeV equivalent). Photomultiplier current readout is provided for source calibration.

During initial operation of the assembled detector, large noise pulses were observed in the photomultipliers. These were largely confined to a few percent of the tubes and had average individual rates of about 0.02 Hz. but a rate over the entire central E-M calorimeter of 30 Hz; these pulses were also associated with noise spikes in the current measurements used for calibration. The problem was traced to microdischarges between tubes and mountings, associated with particular mountings. These discharges have been reduced by wrapping the tubes with 0.005 in. Mylar, and, in some cases, cleaning

the paper-wrapped last inch of the transition pieces. Afterwards, these discharges gave a total trigger rate of 1 Hz.

5. Calibration Systems

Uniformity and calibration considerations were paramount in both design and quality control. Two light fiber mounting holes are provided on each transition piece. Two quartz fibers glued into the transition pieces are terminated with optical connectors which connect to an LED flasher system. An additional fiber mounting hole is provided on an acrylic prism glued to the transverse edge of each waveshifter just above the base plate. A single quartz fiber glued to the prism on the waveshifter is directly bundled to a wedge based xenon flasher system. Both flasher systems are monitored by PIN diodes. A track and pulley mounted on the back of the strip chamber has external access through the 45° end plate. A Co⁶⁰ source with an automatic driver which ran the source on the track was used to set the photomultiplier gains for the first thirteen modules. This single 1 mCi source yielded about 100 nA in each tube of the tower where it was centered after the photomultiplier high voltage was set. Later modules' photomultiplier gains were set with a 3 mCi Cs¹³⁷ source system, chosen for shielding and long lifetime. All modules were eventually outfitted with the Cs¹³⁷ system. This system is permanently mounted with a separate driver and source on each module. The Cs¹³⁷ source also services the hadron calorimeter. The Cs¹³⁷ source is indexed only at limits and is driven at a constant speed allowing a fit to the current profile as the source passes through each tower[7].

Details of the three central E-M calorimeter calibration systems-LED's,

xenon flash, and sources—are described separately[8].

6.Strip Chambers

The strip chambers determine shower position and tranverse development at shower maximum by measurement of the charge deposition on orthogonal strips and wires. Production strip chambers are similar to the prototype[1,3]. The strips are copper backed $\frac{1}{16}$ in. PC boards with through-plated holes for ease of connection. A three piece aluminum extrusion is used as a base to form the cells. Injection molded Delrin pieces are used as wire locators. The strip boards are attached to and insulated from the aluminum by multiple thin layers of epoxy applied to the ribs of the extrusion. A special wire locator allowed the wires to be cut after stringing, dividing each chamber into separate sections. Details of the chambers are listed in Table 4. There is a placement error in locating the chamber in the stack of ± 1 mm. Distortion of the chamber after installation due to unevenness of the stack gives smooth strip gain variations of up to 40%. Detailed maps of each chamber were taken with sources and cosmic rays as part of our testing proceeedures before installation. Applying systematic corrections based on test beam and cosmic ray measurements should result in a resolution of $\pm 10\%$ or better in strip to wire pulse height correlation.

Chamber high voltage is set up to give occasional (few %) channel saturation for 150 GeV/c test beam electrons near normal incidence. For 95%/5% Ar/CO₂ this corresponds to a prompt gain of about 10^3 at 1420 V. Wire and strip readout RABBIT[6] gains are adjusted to give the same dynamic range to both views.

7. Setup and Testing

As central calorimetry modules were completed, they were set up and tested on a cosmic ray test stand; for details, see Reference [9]. Strip chamber gain was set 2.5 times higher than nominal to facilitate observing minimum ionizing signals. A few days' exposure enabled response maps to be studied.

Calibration of each module was performed in the NW beam at Fermilab. This procedure consisted of exposure to 50 GeV/ c electrons, at the center of each tower, correlated to source runs. Several modules were subjected to systematic studies including response maps, energy dependence, pion response, etc. Pairs of modules were studied to reveal effects of the boundary crack. Two extra modules were produced in order to enable systematic studies to continue when fixed target running resumed. The Cs¹³⁷ source system was not available for installation at the beginning of testbeam calibration; consequently, the first seven modules used Co⁶⁰ for their source calibrations. These modules were cross calibrated to Cs¹³⁷ after that source drive was mounted (for details, see [8]). The remaining modules were calibrated with the Cs¹³⁷ source drives.

Module calibration required precise measurement of the module location. This was facilitated by a computer-controlled testbeam "trolley" fixture. This fixture held up to two central wedge modules, two endwall modules, a crack chamber installed between the two wedges on the faces facing the test beam, triggering and veto hodoscopes, and a 1.5 in. aluminum plate in front of the wedges to simulate the superconducting solenoid coil. The fixture rotated about a point such that the test beam entered each tower at normal incidence, and likewise could travel vertically; the motion was directed by

hydraulic pumps extending or contracting piston-driven arms. The momentum of test beam particles was measured by a set of four PWCs—two before and two after the momentum-analyzing dipole located immediately before entrance of the beam into the test beam hall.

8. Performance

The performance of production modules is improved from the prototype due to the improved scintillator and waveshifters[10]. Light yields are typically greater than 100 pe/GeV/tube. Energy resolution for electrons centered in towers (Figure 4) is well described by $\sigma(E)/E = 13.5\%/\sqrt{E \sin \theta}$ (with E in GeV). The energy dependence for electrons from 10 to 100 GeV/c appears to be too large by about 4% at 100 GeV/c; this effect may reflect beamline systematics below 70 GeV/c. The effective attenuation length of the scintillator obtained from the phototube ratios is typically 90 cm. Preliminary studies of response maps over the area of several modules indicate that universal tower maps will be able to reproduce the response over most of the area to within 1%. Energy dependence of the strip chamber response is nonlinear as expected as shown in Figure 5. Position measurement, as shown in Figure 6, is typically ± 2 mm for 50 GeV/c electrons[11].

Results of a study of reproducibility of test beam calibration, performed for each tower of three modules, are shown in Figure 7. Between calibrations each module was rigged out and put in storage. The shift of the distribution corresponds accurately to the decay of the Cs¹³⁷ sources between runs, and the width indicates a reproducibility of about $\pm 0.4\%$. This is discussed in more detail in Reference [8].

Studies of the azimuthal boundary between modules showed a highly irregular response at the wavelength shifter and module skin area. Total calorimeter response ranged from zero to five times the beam energy due to showers producing Čerenkov light in the hadron calorimeter lightguides. These high pulse heights may be suppressed by placing a narrow dense radiator in front of the crack in the limited space outside the solenoid cryostat. A system of 9 radiation length thick uranium bars backed by tagging proportional chambers has been installed on the detector.

9. Conclusion

The central electromagnetic calorimeter for the Collider Detector at Fermilab successfully incorporates a hybrid design using scintillator and wavelength shifter for energy determination and proportional strip chambers for position measurement. All calorimeter modules have been calibrated in a 50 GeV/c electron test beam. The reproducibility of this calibration has been demonstrated to be better than 1%. In addition, systematic studies indicated excellent uniformity in energy and position response over the face of the calorimeter cells. An average energy resolution, $\sigma(E)/E$, of $13.5\%/\sqrt{E \sin \theta}$ and position resolution of 2 mm at 50 GeV has been achieved.

We gratefully acknowledge the support of our colleagues on CDF, members of the Argonne technical staff, the CDF experimental support group, and Fermilab experimental operations crew. This work was supported by the U.S. Department of Energy and the Japanese Ministry of Education, Science and Culture.

* Present Address: AT&T Information Systems, Denver, Colorado 80234

USA

** Present Address: University of California, Santa Barbara, Santa Barbara, California 93106 USA

*** Present Address: Fermi National Accelerator Laboratory, Batavia, Illinois 60510 USA

References

- [1] L. Nodulman, Nucl. Inst. and Meth. **176** (1980) 345.
- [2] *The Collider Detector at Fermilab*, F. Abe et al., submitted to Nucl. Inst. and Meth.
- [3] L. Nodulman et al., Nucl. Inst. and Meth. **204** (1983) 351.
- [4] T. Kamon et al., Nucl. Inst. and Meth. **213** (1983) 261.
- [5] *Phototube Testing for CDF*, T. Devlin et al., submitted to Nucl. Inst. and Meth.
- [6] G. Drake et al., IEEE Trans. Nucl. Sci. **33** (1986) 92;
G. Drake et al., IEEE Trans. Nucl. Sci. **33** (1986) 893;
Front End Electronics: The RABBIT System, G. Drake et al., submitted to Nucl. Inst. and Meth.
- [7] S. Hahn et al., proc. DPF at Santa Fe (1984) 365.
- [8] *Calibration Systems for the CDF Central Electromagnetic Calorimeter*, S. Hahn et al., submitted to Nucl. Inst. and Meth.

- [9] *Cosmic Ray Test of the CDF Central Calorimeters*, R.G. Wagner et al., submitted to Nucl. Inst. and Meth.
- [10] P. Schoessow et al., proc. DPF at Santa Fe (1984) 366.
- [11] *Response Maps of the CDF Central Electromagnetic Calorimeter*, K. Yasuoka et al., submitted to Nucl. Inst. and Meth.

Table 1: Central Electromagnetic Calorimeter Summary.

Modules	
12/arch + 2 spare	50
Length	98 in.
Width	15° in ϕ (17.9 in. at 68+ in. from beamline)
Depth (including base plate)	13.6 in.
Weight	2 metric tons
Towers	
10/module	478
Length	$\Delta\eta$ 0.11 ($\frac{1}{2}$ of width)
Thickness (see Table 2)	18 X_0 , 1 L_{abs} (+coil etc.)
Layers	20-30 lead 21-31 scintillator 1 strip chamber
Lead	$\frac{1}{8}$ in. aluminum clad
Scintillator	5 mm SCSN-38 polystyrene
Wavelength shifter	3 mm Y7 UVA acrylic
Photomultiplier tubes (956 channels)	Hamamatsu R580 ($1\frac{1}{2}$ in.)
Chambers (see Table 4)	
Depth	5.9 X_0 (including coil)
Wire channels (64/module)	3072
Strip channels (128/module)	6130
Angular coverage	
θ	about 39°-141°
ϕ	complete
Pseudorapidity	about ± 1.1
Performance (high = 30+ GeV)	
pe/GeV	100+/tube
Energy resolution σ/E (GeV)	13.5%/ \sqrt{E}
Position resolution (high)	± 2 mm
Strip/wire PH correlation	8-10%
Wire PH resolution (high)	$\pm 25\%$
Hadron rejection (at 50 GeV)	$2-3 \times 10^{-3}$
without strip chamber information	

Table 2: Stack Thickness. Does not include the coil or tracking material. Outer tracking material is approximately $0.11 X_0$ and $0.026 L_{abs}$ divided by $\sin \theta$.

STACK THICKNESS							
TOWER	ANGLE	TO CHAMBER		TOTAL STACK		COIL	
		X_0	L_{abs}	X_0	L_{abs}	X_0	L_{abs}
0	86.3	4.9	0.26	17.9	0.89	0.86	0.20
1	79.15	5.0	0.27	18.2	0.91	0.88	0.20
2	72.2	5.1	0.28	18.2	0.91	0.90	0.20
3	65.65	4.8	0.28	17.8	0.93	0.95	0.21
4	59.75	5.0	0.29	18.0	0.97	1.00	0.23
5	54.5	4.6	0.29	17.7	1.00	1.06	0.24
6	49.85	4.9	0.31	18.1	1.05	1.13	0.26
7	45.9	4.5	0.32	17.7	1.09	1.20	0.27
8	42.2	4.8	0.34	18.0	1.13	1.28	0.29
9	39.9	5.0	0.36	10.	1.	1.34	0.30

Table 3: Salient photomultiplier tube specifications.

PHOTOMULTIPLIER SPECIFICATIONS (1.5 in. dia.)

1. High voltage for current gain of $4. \times 10^5$ less than 1700 V. Total range of required high voltage within 300 V.
2. Bialkali or Multialkali; quantum efficiency for Y7 spectrum greater than 8% (all tubes).
3. No tube dark current above 5 nA for gain of $4. \times 10^5$.
4. Linearity within 1% up to output pulses of 1200 pC.
5. Gain stability after burnin within 1% for 100 hours for anode currents up to 2 μ A, within 2% for 1000 hours at 50 nA.
6. Gain change between 50 nA and 2 μ A within 5%, between 5 nA and 500 nA within 1.5%.
7. Recovery to within 2% of nominal gain within 1 msec after a full scale pulse (1200 pC).
8. Gain dependence on temperature within 0.5% per $^{\circ}$ C.
9. Expected useful lifetime within specifications greater than 50000 hours.

Table 4: Central Electromagnetic Strip Chamber Characteristics. 121.2 cm from the 90° edge of the module corresponds to the boundary between the fifth and sixth scintillator towers.

CHAMBER SPECIFICS

Perpendicular distance to beamline		184 cm
Wire channels (64)		
Extrusion		3 piece aluminum
cell		0.250 in. deep by 0.239 in.
wall		0.047 in. (16.4%)
Wire		0.002 in. Au plated W
Readout		RABBIT
	Split	121.2 cm from 90° edge
	Ganging	pairs except edges (1.453 cm)
	Blocking capacitor	200 pF
Strip channels (128)		
Section 1		6.2–121.2 cm from 90° edge
	strips	69 x 1.67 cm
Section 2		121.2–239.8 cm from 90° edge
	strips	59 x 2.01 cm
Total thickness		0.75 in. 0.069 radiation lengths 0.022 absorption lengths
High voltage		1420 V
Feedin		separate by logical channel
Cable		stripped RG-174
Protection		1 M Ω on board
Gas		95%/5% Ar/CO ₂
Flow		parallel

Figure captions

1. Side view of the stack of lead and scintillator of the central electromagnetic calorimeter (located directly above the floor and rollers). Above the electromagnetic calorimeter is the stack of steel and scintillator, and light pipe fingers, of the hadron calorimeter in the same module. Appropriate substitution of plastic for lead allows the effective thickness in radiation lengths (total and as viewed by the strip chamber) to be nearly independent of angle.
2. Layout of the light-gathering system. The only inaccessible glue joint is the relatively robust 1 in.² attachment of the folded fingers to the rods.
3. Photomultiplier tube base circuit. Note the resistive protection of the internal ground and the diode protection circuit.
4. Central electromagnetic calorimeter energy resolution as a function of the energy for both phototubes of tower 1 of a typical calorimeter module. The large errors at higher values of $E^{-1/2}$ are due to lower beamline delivery of low energy electrons.
5. Strip chamber pulse height energy dependence. The pulse height per beam momentum is scaled to 1.0 at 50 GeV/ c . The falloff is as expected for the depth of the chamber. The error bars correspond to the rms width of the pulse height distributions.
6. Strip chamber position measurement near 90°. Strip view (squares) measurement scales up as $\sin^{-1} \theta$ away from 90°.

7. Calibration reproducibility. The difference in beam to Cs^{137} source ratio for each tube is plotted for successive calibration procedures, about 5 weeks apart, for three modules. The deviation of the centroid from zero corresponds accurately to the source decay.

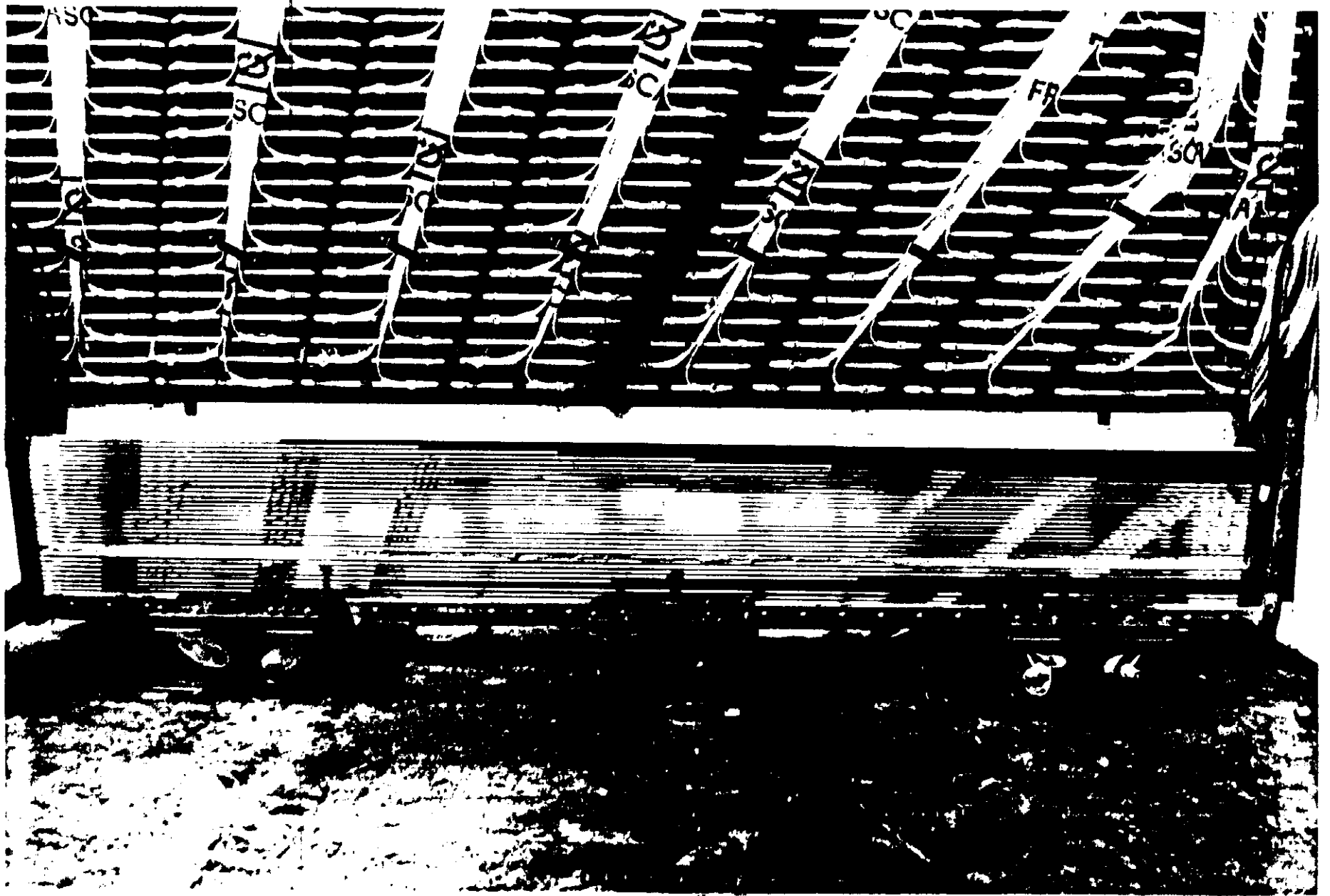


Fig. 1

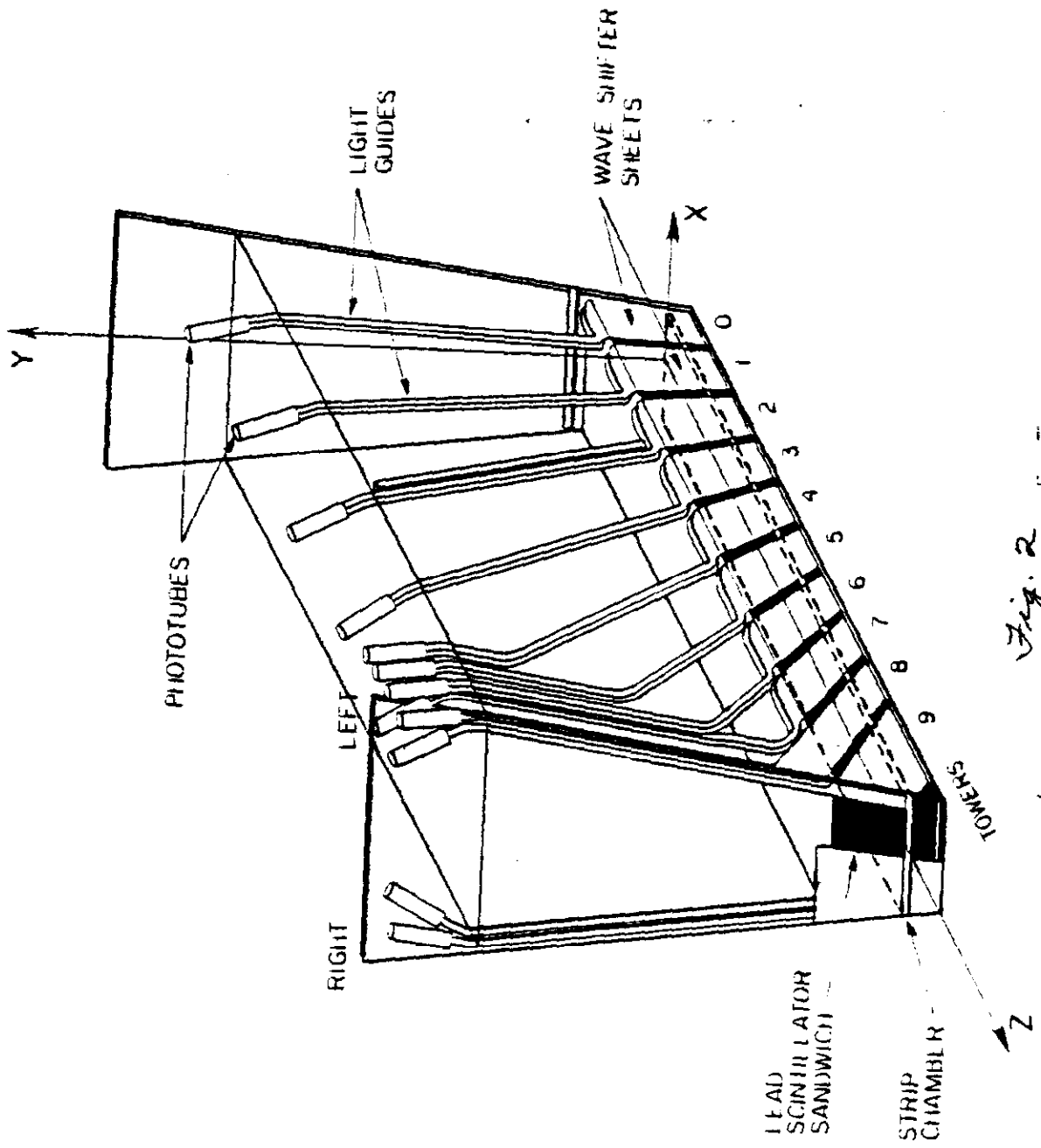


Fig. 2

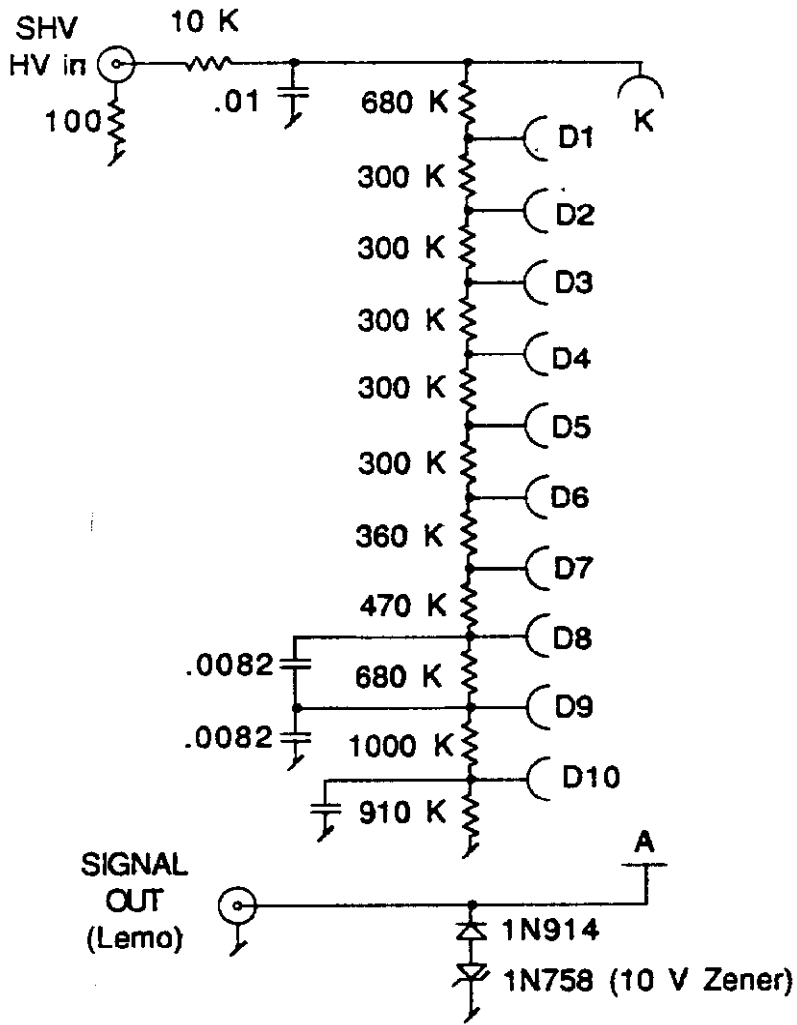


Fig. 3

CDF Central E-M Calorimeter

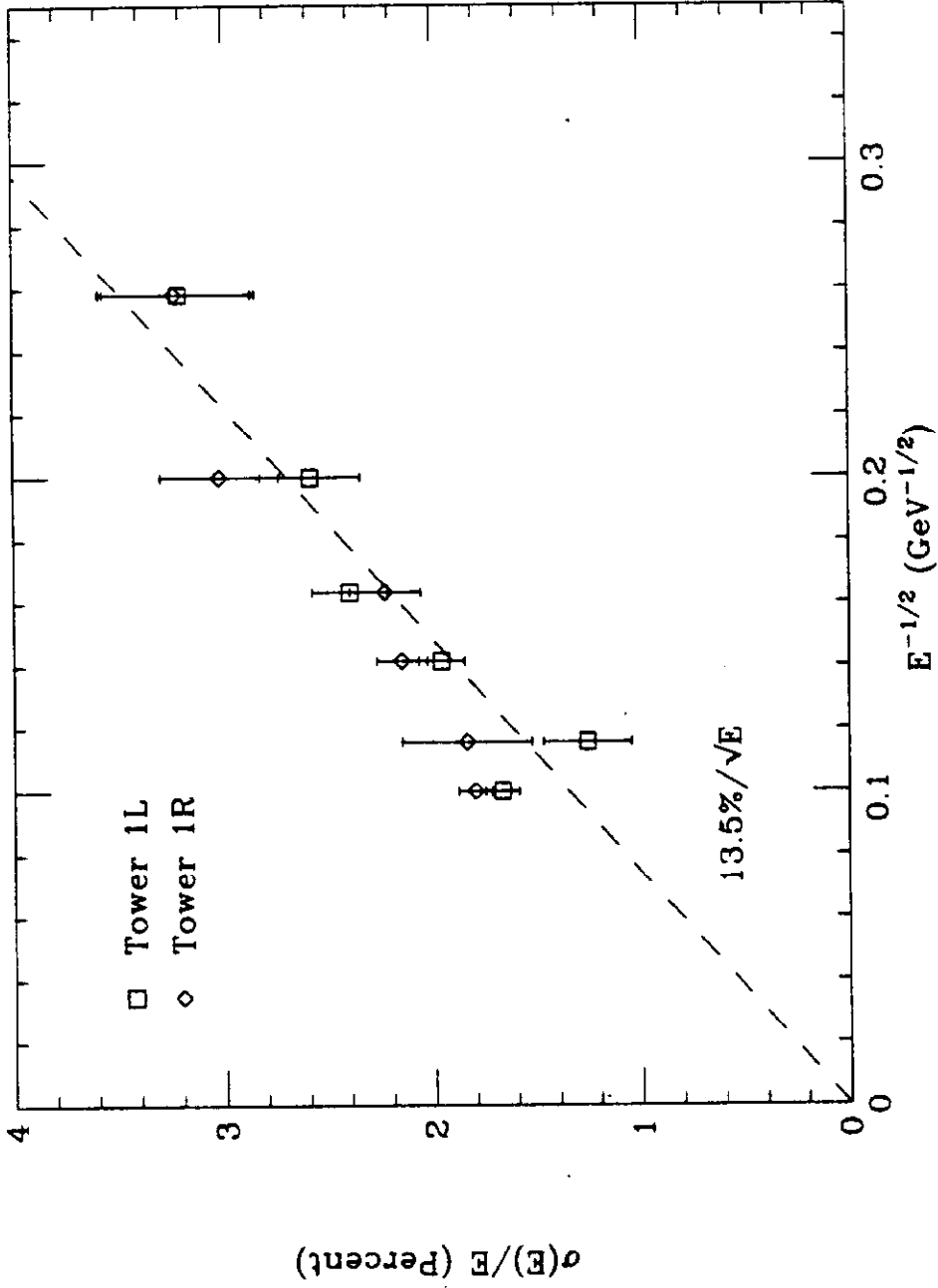


Fig. 4

Strip Chamber Energy Dependence

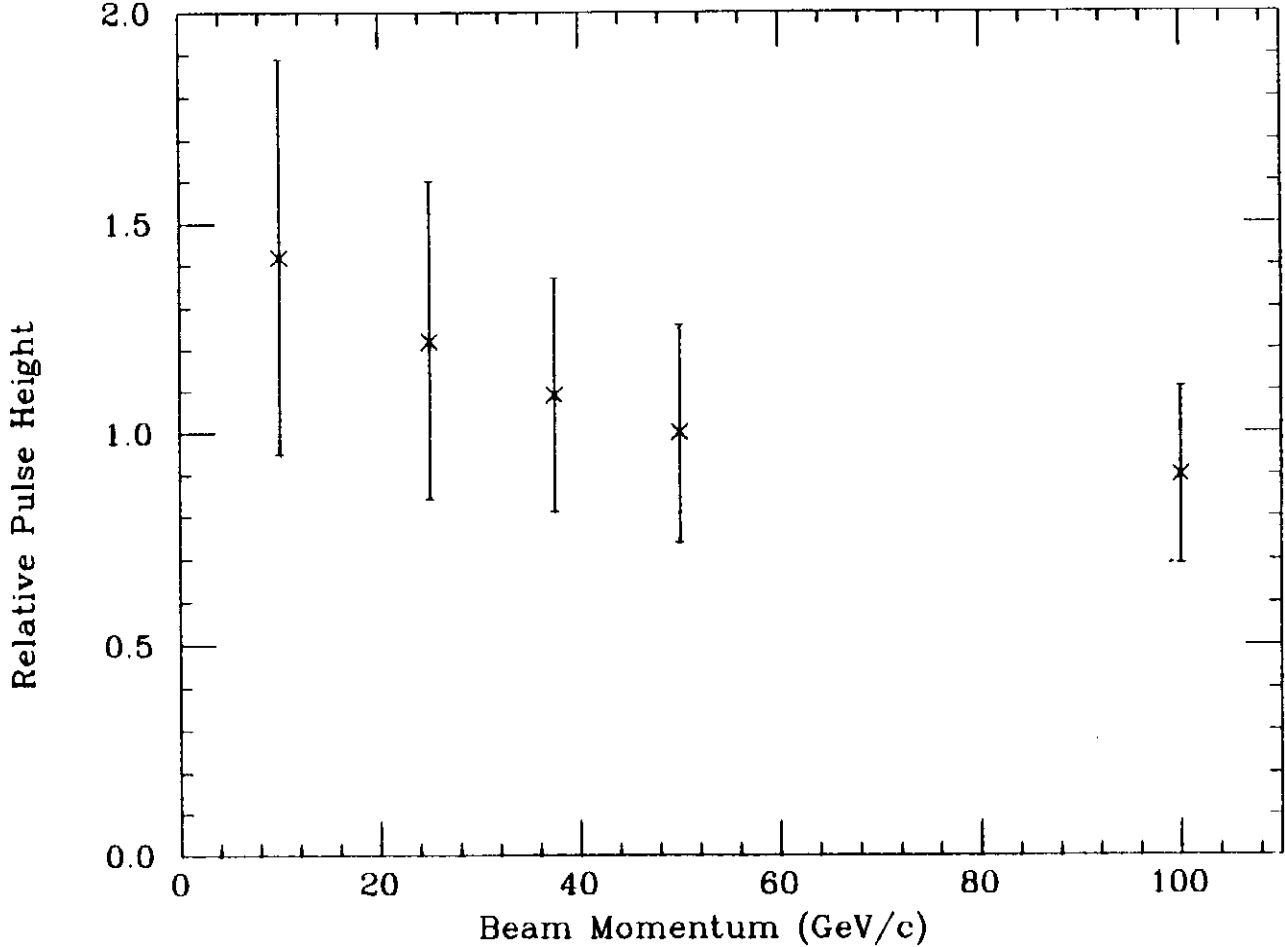


Fig. 5

Strip Chamber Position Resolution

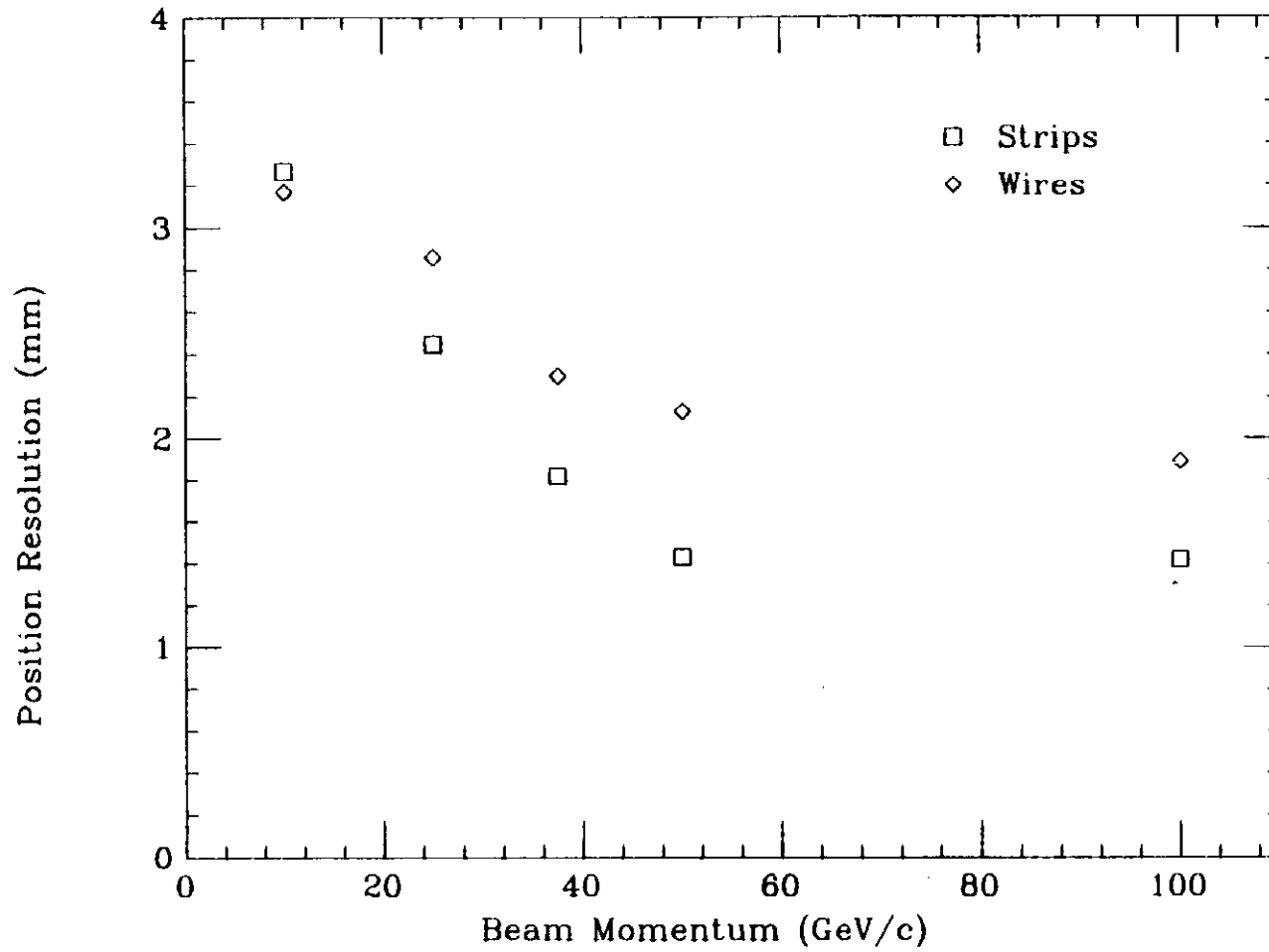


Fig. 6

E-M calibration reproducibility

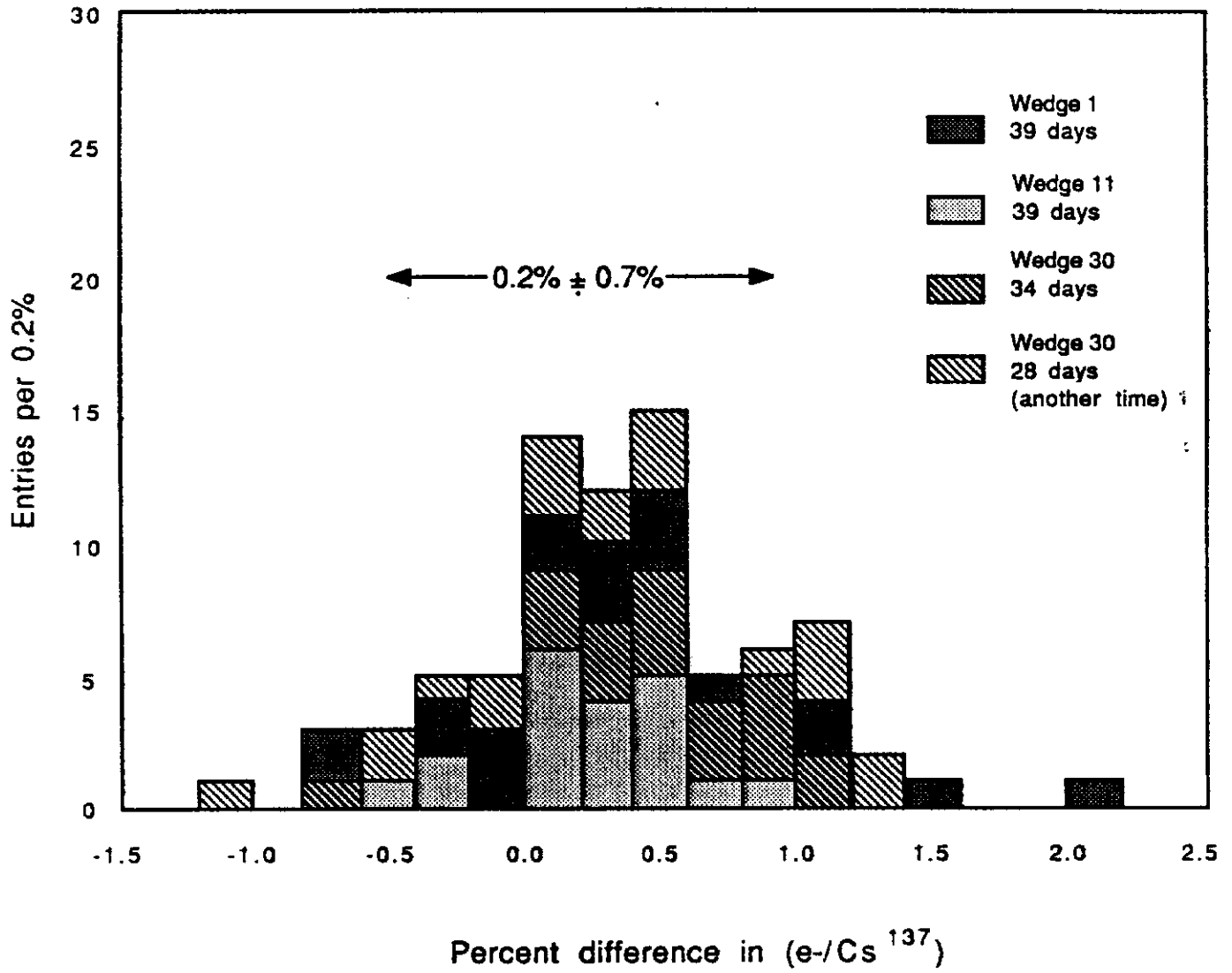


Fig. 7